
MagNet: A Neural Network for Directed Graphs

Anonymous Author(s)
Affiliation
Address
email

Abstract

1 The prevalence of graph-based data has spurred the rapid development of graph
2 neural networks (GNNs) and related machine learning algorithms. Yet, despite the
3 many datasets naturally modeled as directed graphs, including citation, website,
4 and traffic networks, the vast majority of this research focuses on undirected graphs.
5 In this paper, we propose *MagNet*, a spectral GNN for directed graphs based on a
6 complex Hermitian matrix known as the magnetic Laplacian. This matrix encodes
7 undirected geometric structure in the magnitude of its entries and directional
8 information in their phase. A “charge” parameter attunes spectral information to
9 variation among directed cycles. We apply our network to a variety of directed
10 graph node classification and link prediction tasks showing that MagNet performs
11 well on all tasks and that its performance exceeds all other methods on a majority
12 of such tasks. The underlying principles of MagNet are such that it can be adapted
13 to other spectral GNN architectures.

14 1 Introduction

15 Endowing a collection of objects with a graph structure allows one to encode pairwise relationships
16 among its elements. These relations often possess a natural notion of direction. For example, the
17 WebKB dataset [32] contains a list of university websites with associated hyperlinks. In this context,
18 one website might link to a second without a reciprocal link to the first. Such datasets are naturally
19 modeled by *directed graphs*. In this paper, we introduce *MagNet*, a graph convolutional neural
20 network for directed graphs based on the magnetic Laplacian.

21 Most graph neural networks fall into one of two families, *spectral networks* or *spatial networks*.
22 Spatial methods define graph convolution as a localized averaging operation with iteratively learned
23 weights. Spectral networks, on the other hand, define convolution on graphs via the eigendecomposi-
24 tion of the (normalized) graph Laplacian. The eigenvectors of the graph Laplacian assume the role
25 of Fourier modes, and convolution is defined as entrywise multiplication in the Fourier basis. For a
26 comprehensive review of both spatial and spectral networks, we refer the reader to [42] and [40].

27 Many spatial graph CNNs have natural extensions to directed graphs. However, it is common for
28 these methods to preprocess the data by symmetrizing the adjacency matrix, effectively creating
29 an undirected graph. For example, while [38] explicitly notes that their network is well-defined on
30 directed graphs, their experiments treat all citation networks as undirected for improved performance.

31 Extending spectral methods to directed graphs is not straightforward since the adjacency matrix is
32 asymmetric and, thus, there is no obvious way to define a symmetric, real-valued Laplacian with a
33 full set of real eigenvalues that uniquely encodes any directed graph. We overcome this challenge
34 by constructing a network based on the magnetic Laplacian $L^{(g)}$ defined in Section 2. Unlike the
35 directed graph Laplacians used in works such as [26, 30, 36, 37], the magnetic Laplacian is not a
36 real-valued symmetric matrix. Instead, it is a *complex-valued Hermitian* matrix that encodes the
37 fundamentally asymmetric nature of a directed graph via the complex phase of its entries.

38 Since $\mathbf{L}^{(q)}$ is Hermitian, the spectral theorem implies it has an orthonormal basis of complex
 39 eigenvectors corresponding to real eigenvalues. Moreover, Theorem 1, stated in Section 5 of the
 40 supplement, shows that $\mathbf{L}^{(q)}$ is positive semidefinite, similar to the traditional Laplacian. Setting
 41 $q = 0$ is equivalent to symmetrizing the adjacency matrix and no importance is given to directional
 42 informatio. When $q = .25$, on the other hand, we have that $\mathbf{L}^{(.25)}(u, v) = -\mathbf{L}^{(.25)}(v, u)$ whenever
 43 there is an edge from u to v but not from v to u . Different values of q highlight different graph motifs
 44 [16, 17, 19, 29], and therefore the optimal choice of q varies. Learning the appropriate value of q
 45 from data allows MagNet to adaptively incorporate directed information. We also note that $\mathbf{L}^{(q)}$ has
 46 been applied to graph signal processing [18], community detection [17], and clustering [10, 16, 15].

47 In Section 3, we show how the networks constructed in [6, 13, 22] can be adapted to directed graphs
 48 by incorporating complex Hermitian matrices, such as the magnetic Laplacian. When $q = 0$, we
 49 effectively recover the networks constructed in those previous works. Therefore, our work generalizes
 50 these networks in a way that is suitable for directed graphs. Our method is very general and is not
 51 tied to any particular choice of network architecture. Indeed, the main ideas of this work could be
 52 adapted to nearly any spectral network.

53 In Section 4, we summarize related work on directed graph neural networks as well as other papers
 54 studying the magnetic Laplacian and its applications in data science. In Section 5, we apply our
 55 network to node classification and link prediction tasks. We compare against several spectral and
 56 spatial methods as well as networks designed for directed graphs. We find that MagNet obtains
 57 the best or second-best performance on five out of six node-classification tasks and has the best
 58 performance on seven out of eight link-prediction tasks tested on real-world data, in addition to
 59 providing excellent node-classification performance on difficult synthetic data. We also provide a
 60 supplementary document with full implementation details, theoretical results concerning the magnetic
 61 Laplacian, extended examples, and further numerical details.

62 2 The magnetic Laplacian

63 Spectral graph theory has been remarkably successful in relating geometric characteristics of undi-
 64 rected graphs to properties of eigenvectors and eigenvalues of graph Laplacians and related matrices.
 65 For example, the tasks of optimal graph partitioning, sparsification, clustering, and embedding may
 66 be approximated by eigenvectors corresponding to small eigenvalues of various Laplacians (see, e.g.,
 67 [9, 34, 2, 35, 11]). Similarly, the graph signal processing research community leverages the full set of
 68 eigenvectors to extend the Fourier transform to these structures [31]. Furthermore, numerous papers
 69 [6, 13, 22] have shown that this eigendecomposition can be used to define neural networks on graphs.
 70 In this section, we provide the background needed to extend these constructions to directed graphs
 71 via complex Hermitian matrices such as the magnetic Laplacian.

72 We let $G = (V, E)$ be a directed graph where V is a set of N vertices and $E \subseteq V \times V$ is a set of
 73 directed edges. If $(u, v) \in E$, then we say there is an edge from u to v . For the sake of simplicity, we
 74 will focus on the case where the graph is unweighted and has no self-loops, i.e., $(v, v) \notin E$, but our
 75 methods have natural extensions to graphs with self-loops and/or weighted edges. If both $(u, v) \in E$
 76 and $(v, u) \in E$, then one may consider this pair of directed edges as a single undirected edge.

77 A directed graph can be described by an adjacency matrix $(\mathbf{A}(u, v))_{u, v \in V}$ where $\mathbf{A}(u, v) = 1$ if
 78 $(u, v) \in E$ and $\mathbf{A}(u, v) = 0$ otherwise. Unless G is undirected, \mathbf{A} is not symmetric, and, indeed, this
 79 is the key technical challenge in extending spectral graph neural networks to directed graphs. In the
 80 undirected case, where the adjacency matrix \mathbf{A} is symmetric, the (unnormalized) graph Laplacian
 81 can be defined by $\mathbf{L} = \mathbf{D} - \mathbf{A}$, where \mathbf{D} is a diagonal degree matrix. It is well-known that \mathbf{L} is
 82 a symmetric, positive-semidefinite matrix and therefore has an orthonormal basis of eigenvectors
 83 associated with non-negative eigenvalues. However, when \mathbf{A} is asymmetric, direct attempts to
 84 define the Laplacian this way typically yield complex eigenvalues. This impedes the straightforward
 85 extension of classical methods of spectral graph theory and graph signal processing to directed graphs.

86 A key point of this paper is to represent the directed graph through a complex Hermitian matrix
 87 \mathcal{L} such that: (1) the magnitude of $\mathcal{L}(u, v)$ indicates the presence of an edge, but not its direction;
 88 and (2) the phase of $\mathcal{L}(u, v)$ indicates the direction of the edge, or if the edge is undirected. Such
 89 matrices have been explored in the directed graph literature (see Section 4), but not in the context of
 90 graph neural networks. They have several advantages over their real-valued matrix counterparts. In
 91 particular, a single symmetric real-valued matrix will not uniquely represent a directed graph. Instead,

92 one must use several matrices, as in [37], but this increases the complexity of the resulting network.
 93 Alternatively, one can work with an asymmetric, real-valued matrix, such as the adjacency matrix or
 94 the random walk matrix. However, the spatial graph filters that result from such matrices are typically
 95 limited by the fact that they can only aggregate information from the vertices that can be reached
 96 in one hop from a central vertex, but ignore the equally important subset of vertices that can reach
 97 the central vertex in one hop. Complex Hermitian matrices, however, lead to filters that aggregate
 98 information from both sets of vertices. Finally, one could use a real-valued skew-symmetric matrix
 99 but such matrices do not generalize well to graphs with both directed and undirected edges.

100 The optimal choice of complex Hermitian matrix is an open question. Here, we utilize a parameterized
 101 family of magnetic Laplacians, which have proven to be useful in other data-driven contexts [17, 10,
 102 16, 15]. We first define the symmetrized adjacency matrix and corresponding degree matrix by,

$$\mathbf{A}_s(u, v) := \frac{1}{2}(\mathbf{A}(u, v) + \mathbf{A}(v, u)), \quad 1 \leq u, v \leq N, \quad \mathbf{D}_s(u, u) := \sum_{v \in V} \mathbf{A}_s(u, v), \quad 1 \leq u \leq N,$$

103 with $\mathbf{D}_s(u, v) = 0$ for $u \neq v$. We capture directional information via a phase matrix,¹ $\Theta^{(q)}$,

$$\Theta^{(q)}(u, v) := 2\pi q(\mathbf{A}(u, v) - \mathbf{A}(v, u)), \quad q \geq 0,$$

104 where $\exp(i\Theta^{(q)})$ is defined component-wise by $\exp(i\Theta^{(q)})(u, v) := \exp(i\Theta^{(q)}(u, v))$. Letting \odot
 105 denotes componentwise multiplication, we define the complex Hermitian adjacency matrix $\mathbf{H}^{(q)}$ by

$$\mathbf{H}^{(q)} := \mathbf{A}_s \odot \exp(i\Theta^{(q)}).$$

106 Since $\Theta^{(q)}$ is skew-symmetric, $\mathbf{H}^{(q)}$ is Hermitian. When $q = 0$, we have $\Theta^{(0)} = \mathbf{0}$ and so
 107 $\mathbf{H}^{(0)} = \mathbf{A}_s$. This effectively corresponds to treating the graph as undirected. For $q \neq 0$, the phase of
 108 $\mathbf{H}^{(q)}$ encodes edge direction. For example, if there is an edge from u to v but not from v to u we have

$$\mathbf{H}^{(0.25)}(u, v) = \frac{i}{2} = -\mathbf{H}^{(0.25)}(v, u).$$

109 Thus, in this setting, an edge from u to v is treated as the opposite of an edge from v to u . On
 110 the other hand, if $(u, v), (v, u) \in E$ (which can be interpreted as a single undirected edge), then
 111 $\mathbf{H}^{(q)}(u, v) = \mathbf{H}^{(q)}(v, u) = 1$, and we see the phase, $\Theta^{(q)}(u, v) = 0$, encodes the lack of direction in
 112 the edge. For the rest of this paper, we will assume that q lies in between these two extreme values,
 113 i.e., $0 \leq q \leq .25$. We define the normalized and unnormalized and magnetic Laplacians by

$$\mathbf{L}_U^{(q)} := \mathbf{D}_s - \mathbf{H}^{(q)} = \mathbf{D}_s - \mathbf{A}_s \odot \exp(i\Theta^{(q)}), \quad \mathbf{L}_N^{(q)} := \mathbf{I} - \left(\mathbf{D}_s^{-1/2} \mathbf{A}_s \mathbf{D}_s^{-1/2} \right) \odot \exp(i\Theta^{(q)}). \quad (1)$$

114 Note that when G is undirected, $\mathbf{L}_U^{(q)}$ and $\mathbf{L}_N^{(q)}$ reduce to the standard undirected Laplacians.

115 $\mathbf{L}_U^{(q)}$ and $\mathbf{L}_N^{(q)}$ are Hermitian. Theorem 1 (see Section 5 of the supplement) shows they are positive-
 116 semidefinite and thus are diagonalized by an orthonormal basis of complex eigenvectors $\mathbf{u}_1, \dots, \mathbf{u}_N$
 117 associated to real, nonnegative eigenvalues $\lambda_1, \dots, \lambda_N$. Similar to the traditional normalized Lapla-
 118 cian, Theorem 2 (see Section 5 of the supplement) shows that the eigenvalues of $\mathbf{L}_N^{(q)}$ lie in $[0, 2]$,
 119 and we may factor $\mathbf{L}_N^{(q)} = \mathbf{U}\mathbf{\Lambda}\mathbf{U}^\dagger$, where \mathbf{U} is the $N \times N$ matrix whose k -th column is \mathbf{u}_k , $\mathbf{\Lambda}$ is
 120 the diagonal matrix with $\mathbf{\Lambda}(k, k) = \lambda_k$, and \mathbf{U}^\dagger is the conjugate transpose of \mathbf{U} (a similar formula
 121 holds for $\mathbf{L}_U^{(q)}$). The magnetic Laplacian encodes in its eigenvectors and eigenvalues. In the directed
 122 star graph, for example, directional information is contained in the eigenvectors only, whereas the
 123 eigenvalues are invariant directionality. On the other hand, for the directed cycle graph the magnetic
 124 Laplacian encodes the directed nature of the graph solely in its spectrum (see Section 6 of the
 125 supplement). In general, both the eigenvectors and eigenvalues may contain important information.
 126 In Section 3, we will introduce MagNet, a network designed to leverage this spectral information.

¹Our definition of $\Theta^{(q)}$ coincides with that used in [18]. However, another definition (differing by a minus sign) also appears in the literature. These resulting magnetic Laplacians have the same eigenvalues and the corresponding eigenvectors are complex conjugates of one another. Therefore, this difference does not affect the performance of our network since our final layer separates the real and imaginary parts before multiplying by a trainable weight matrix (see Section 3 for details on the network structure).

127 **3 MagNet**

128 Most graph neural network architectures can be described as being either *spectral* or *spatial*. Spatial
 129 networks such as [38, 20, 1, 14] typically extend convolution to graphs by performing a weighted
 130 average of features over neighborhoods $\mathcal{N}(u) = \{v : (u, v) \in E\}$. These neighborhoods are
 131 well-defined even when E is not symmetric, so spatial methods typically have natural extensions
 132 to directed graphs. However, such simplistic extensions may miss important information in the
 133 directed graph. For example, filters defined using $\mathcal{N}(u)$ are not capable of assimilating the equally
 134 important information contained in $\{v : (v, u) \in E\}$. Alternatively, these methods may also use the
 135 symmetrized adjacency matrix, but they cannot learn to balance directed and undirected approaches.

136 In this section, we show how to extend spectral methods to directed graphs using the magnetic
 137 Laplacian introduced in Section 2. To highlight the flexibility of our approach, we show how three
 138 spectral graph neural network architectures can be adapted to incorporate the magnetic Laplacian.
 139 Our approach is very general, and so for most of this section, we will perform our analysis for a
 140 general complex Hermitian, positive semidefinite matrix. However, we view the magnetic Laplacian
 141 as our primary object of interest (and use it in all of our experiments) because of the large body of
 142 literature studying its spectral properties and applying it to data science (see Section 4).

143 **3.1 Spectral convolution via the magnetic Laplacian**

144 In this section, we let \mathcal{L} denote a Hermitian, positive semidefinite matrix, such as the normalized or
 145 unnormalized magnetic Laplacian introduced in Section 2, on a directed graph $G = (V, E)$, $|V| = N$.
 146 We let $\mathbf{u}_1, \dots, \mathbf{u}_N$ be an orthonormal basis of eigenvectors for \mathcal{L} and let \mathbf{U} be the $N \times N$ matrix
 147 whose k -th column is \mathbf{u}_k . We define the directed graph Fourier transform for a signal $\mathbf{x} : V \rightarrow \mathbb{C}$ by
 148 $\hat{\mathbf{x}} = \mathbf{U}^\dagger \mathbf{x}$, so that $\hat{\mathbf{x}}(k) = \langle \mathbf{x}, \mathbf{u}_k \rangle$. We regard the eigenvectors $\mathbf{u}_1, \dots, \mathbf{u}_N$ as the generalizations of
 149 discrete Fourier modes to directed graphs. Since \mathbf{U} is unitary, we have the Fourier inversion formula

$$\mathbf{x} = \mathbf{U}\hat{\mathbf{x}} = \sum_{k=1}^N \hat{\mathbf{x}}(k)\mathbf{u}_k. \quad (2)$$

150 In Euclidean space, convolution corresponds to pointwise multiplication in the Fourier basis. Thus,
 151 we define the convolution of \mathbf{x} with a filter \mathbf{y} in the Fourier domain by $\hat{\mathbf{y}} * \hat{\mathbf{x}}(k) = \hat{\mathbf{y}}(k)\hat{\mathbf{x}}(k)$. By (2),
 152 this implies $\mathbf{y} * \mathbf{x} = \mathbf{U}\text{Diag}(\hat{\mathbf{y}})\hat{\mathbf{x}} = (\mathbf{U}\text{Diag}(\hat{\mathbf{y}})\mathbf{U}^\dagger)\mathbf{x}$, and so we say \mathbf{Y} is a convolution matrix if

$$\mathbf{Y} = \mathbf{U}\mathbf{\Sigma}\mathbf{U}^\dagger, \quad (3)$$

153 for a diagonal matrix $\mathbf{\Sigma}$. This is the natural generalization of the class of convolutions used in [6].

154 Next, following [13] (see also [21]), we show that a spectral network can be implemented in the
 155 spatial domain via polynomials of \mathcal{L} by having $\mathbf{\Sigma}$ be a polynomial of $\mathbf{\Lambda}$ in (3). This reduces the
 156 number of trainable parameters to prevent overfitting, avoids explicit diagonalization of the matrix \mathcal{L} ,
 157 (which is expensive for large graphs), and improves stability to perturbations [24]. As in [13], we
 158 define a normalized eigenvalue matrix, with entries in $[-1, 1]$, by $\tilde{\mathbf{\Lambda}} = \frac{2}{\lambda_{\max}}\mathbf{\Lambda} - \mathbf{I}$ and assume

$$\mathbf{\Sigma} = \sum_{k=0}^K \theta_k T_k(\tilde{\mathbf{\Lambda}}),$$

159 for some real-valued $\theta_1, \dots, \theta_k$, where for $k \geq 0$, T_k is the Chebyshev polynomial defined by
 160 $T_0(x) = 1, T_1(x) = x$, and $T_k(x) = 2xT_{k-1}(x) + T_{k-2}(x)$ for $k \geq 2$. One can use the fact that
 161 $(\mathbf{U}\tilde{\mathbf{\Lambda}}\mathbf{U}^\dagger)^k = \mathbf{U}\tilde{\mathbf{\Lambda}}^k\mathbf{U}^\dagger$ to see

$$\mathbf{Y}\mathbf{x} = \mathbf{U} \sum_{k=0}^K \theta_k T_k(\tilde{\mathbf{\Lambda}})\mathbf{U}^\dagger \mathbf{x} = \sum_{k=0}^K \theta_k T_k(\tilde{\mathcal{L}})\mathbf{x}, \quad (4)$$

162 where, analogous to $\tilde{\mathbf{\Lambda}}$, we define $\tilde{\mathcal{L}} := \frac{2}{\lambda_{\max}}\mathcal{L} - \mathbf{I}$. It is important to note that, due to the complex
 163 Hermitian structure of $\tilde{\mathcal{L}}$, the value $\mathbf{Y}\mathbf{x}(u)$ aggregates information both from the values of \mathbf{x} on
 164 $\mathcal{N}_k(u)$, the k -hop neighborhood of u , and the values of \mathbf{x} on $\{v : \text{dist}(v, u) \leq k\}$, which consists
 165 of those of vertices that can reach u in k -hops. While in an undirected graph these two sets of

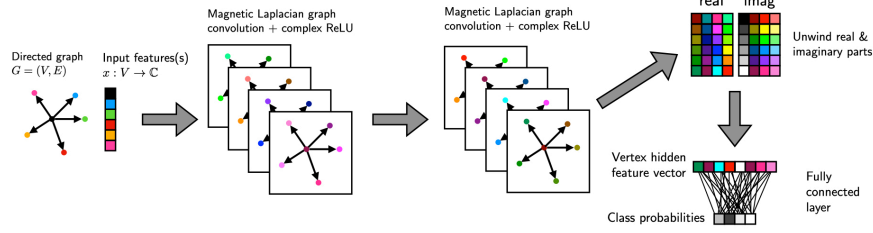


Figure 1: MagNet ($L = 2$) applied to node classification. After two complex convolutional layers, we unwind the real and imaginary parts of our feature matrix and apply a fully connected layer.

166 vertices are the same, that is not the case for general directed graphs. Furthermore, due to the
 167 difference in phase between an edge (u, v) and an edge (v, u) , the filter matrix \mathbf{Y} is also capable of
 168 aggregating information from these two sets in different ways. This capability is in contrast to any
 169 single, symmetric, real-valued matrix, as well as any matrix that encodes just $\mathcal{N}(u)$.

170 To obtain a network similar to [22], we set $K = 1$, assume that $\mathcal{L} = \mathbf{L}_N^{(q)}$, using $\lambda_{\max} \leq 2$ (see
 171 Theorem 2 in Section 5 of the supplement) make the approximation $\lambda_{\max} \approx 2$, and set $\theta_1 = -\theta_0$.
 172 With this, we obtain

$$\mathbf{Y}\mathbf{x} = \theta_0(\mathbf{I} + (\mathbf{D}_s^{-1/2} \mathbf{A}_s \mathbf{D}_s^{-1/2}) \odot \exp(i\Theta^{(q)}))\mathbf{x}.$$

173 As in [22], we substitute $(\mathbf{I} + (\mathbf{D}_s^{-1/2} \mathbf{A}_s \mathbf{D}_s^{-1/2}) \odot \exp(i\Theta^{(q)})) \rightarrow \tilde{\mathbf{D}}_s^{-1/2} \tilde{\mathbf{A}}_s \tilde{\mathbf{D}}_s^{-1/2} \exp(i\Theta^{(q)})$.
 174 This renormalization helps avoid instabilities arising from vanishing/exploding gradients and yields

$$\mathbf{Y}\mathbf{x} = \theta_0 \tilde{\mathbf{D}}_s^{-1/2} \tilde{\mathbf{A}}_s \tilde{\mathbf{D}}_s^{-1/2} \odot \exp(i\Theta^{(q)}), \quad (5)$$

175 where $\tilde{\mathbf{A}}_s = \mathbf{A}_s + \mathbf{I}$ and $\tilde{\mathbf{D}}_s(i, i) = \sum_j \tilde{\mathbf{A}}_s(i, j)$.

176 3.2 The MagNet architecture

177 We now define our network. Let L be the number of convolution layers in our network, and let $\mathbf{X}^{(0)}$
 178 be an $N \times F_0$ input feature matrix with columns $\mathbf{x}_1^{(0)}, \dots, \mathbf{x}_{F_0}^{(0)}$. Since our filters are complex, we use
 179 a complex version of ReLU defined by $\sigma(z) = z$, if $-\pi/2 \leq \arg(z) < \pi/2$, and $\sigma(z) = 0$ otherwise
 180 (where $\arg(z)$ is the complex argument of $z \in \mathbb{C}$). We let F_ℓ be the number of channels in layer ℓ ,
 181 and for $1 \leq \ell \leq L$, $1 \leq i \leq F_{\ell-1}$, and $1 \leq j \leq F_\ell$, we let $\mathbf{Y}_{ij}^{(\ell)}$ be a convolution matrix defined in
 182 the sense of either (3), (4), or (5). To obtain the layer ℓ channels from the layer $\ell - 1$ channels, we
 183 define the matrix $\mathbf{X}^{(\ell)}$ with columns $\mathbf{x}_1^{(\ell)}, \dots, \mathbf{x}_{F_\ell}^{(\ell)}$ as:

$$\mathbf{x}_j^{(\ell)} = \sigma \left(\sum_{i=1}^{F_{\ell-1}} \mathbf{Y}_{ij}^{(\ell)} \mathbf{x}_i^{(\ell-1)} \right). \quad (6)$$

184 In matrix form we write $\mathbf{X}^{(\ell)} = \mathbf{Z}^{(\ell)} (\mathbf{X}^{(\ell-1)})$, where $\mathbf{Z}^{(\ell)}$ is a hidden layer of the form (6).

185 After the convolutional layers, we unwind the complex $N \times F_L$ matrix $\mathbf{X}^{(L)}$ into a real-valued
 186 $N \times 2F_L$ matrix, apply a linear layer, consisting of right-multiplication by a $2F_L \times n_c$ weight matrix
 187 $\mathbf{W}^{(L+1)}$ (where n_c is the number of classes) and apply softmax. In our experiments, we set $L = 2$ or
 188 3. When $L = 2$, our network applied to node classification, as illustrated in Figure 1, is given by

$$\text{softmax}(\text{unwind}(\mathbf{Z}^{(2)}(\mathbf{Z}^{(1)}(\mathbf{X}^{(0)})))\mathbf{W}^{(3)}).$$

189 For link-prediction, we apply the same method through the unwind layer, but then subtract the rows
 190 corresponding to pairs of nodes to obtain the edge features.

191 4 Related work

192 In Section 4.1, we describe other graph neural networks designed specifically for directed graphs.
 193 Notably, none of these methods encode directionality with complex numbers, instead opting for real-
 194 valued, symmetric matrices. In Section 4.2, we review other work studying the magnetic Laplacian

195 which has been studied for several decades and lately has garnered interest in the network science
 196 and graph signal processing communities. However, to the best of our knowledge, this is the first
 197 work to use it to construct a graph neural network. We also note there are numerous approaches to
 198 graph signal processing on directed graphs. Many of these rely on a natural analog of Fourier modes.
 199 These Fourier modes are typically defined through either a factorization of a graph shift operator or
 200 by solving an optimization problem. For further review, we refer the reader to [27].

201 4.1 Neural networks for directed graphs

202 In [26], the authors construct a directed Laplacian, via identities involving the random walk matrix
 203 and its stationary distribution $\mathbf{\Pi}$. When G is undirected, one can use the fact that $\mathbf{\Pi}$ is proportional
 204 to the degree vector to verify this directed Laplacian reduces to the standard normalized graph
 205 Laplacian. However, this method requires G to be strongly connected, unlike MagNet. The authors
 206 of [37] use a first-order proximity matrix \mathbf{A}_F (equivalent to \mathbf{A}_s here), as well as two second-order
 207 proximity matrices $\mathbf{A}_{S_{in}}$ and $\mathbf{A}_{S_{out}}$. $\mathbf{A}_{S_{in}}$ is defined by $\mathbf{A}_{S_{in}}(u, v) \neq 0$ if there exists a w such that
 208 $(w, u), (w, v) \in E$, and $\mathbf{A}_{S_{out}}$ is defined analogously. These three matrices collectively describe and
 209 distinguish the neighborhood of each vertex and those vertices that can reach a vertex in a single
 210 hop. The authors construct three different Laplacians and use a fusion operator to share information
 211 across channels. Similarly, inspired by [3], in [30], the authors consider several different symmetric
 212 Laplacian matrices corresponding to a number of different graph motifs.

213 The method of [36] builds upon the ideas of both [26] and [37] and considers a directed Laplacian
 214 similar to the one used in [26], but with a PageRank matrix in place of the random-walk matrix.
 215 This allows for applications to graphs which are not strongly connected. Similar to [37], they use
 216 higher-order receptive fields (analogous to the second-order adjacency matrices discussed above) and
 217 an inception module to share information between receptive fields of different orders. We also note
 218 [23], which uses an approach based on PageRank in the spatial domain.

219 4.2 Related work on the magnetic Laplacian and Hermitian adjacency matrices

220 The magnetic Laplacian has been studied since at least [25]. The name originates from its interpreta-
 221 tion as a quantum mechanical Hamiltonian of a particle under magnetic flux. Early works focused on
 222 d -regular graphs, where the eigenvectors of the magnetic Laplacian are equivalent to those of the Her-
 223 mitian adjacency matrix. [19], for example, show that using a complex-valued Hermitian adjacency
 224 matrix rather than the symmetrized adjacency matrix reduces the number of small, non-isomorphic
 225 cospectral graphs. Topics of current research into Hermitian adjacency matrices include clustering
 226 tasks [12] and the role of the parameter q [29].

227 The magnetic Laplacian is also the subject of ongoing research in graph signal processing [18],
 228 community detection [17], and clustering [10, 16, 15]. For example, [16] uses the phase of the
 229 eigenvectors to construct eigenmap embeddings analogous to [2]. The role of q is highlighted in the
 230 works of [16, 17, 19, 29], which show how particular choices of q may highlight various graph motifs.
 231 In our context, this indicates that q should be carefully tuned via cross-validation. Lastly, we note that
 232 numerous other directed graph Laplacians have been studied and applied to data science [7, 8, 39].
 233 However, as alluded to in Section 2, these methods typically do not use complex Hermitian matrices.

234 5 Numerical experiments

235 We test the performance of MagNet for node classification and link prediction on a variety of
 236 benchmark datasets as well as a directed stochastic block model.

237 5.1 Datasets

238 5.1.1 Directed Stochastic Block Model

239 We construct a directed stochastic block (DSBM) model as follows. First we divide N vertices into
 240 n_c clusters C_1, \dots, C_{n_c} . We, define $\{\alpha_{i,j}\}_{1 \leq i,j \leq n_c}$ to be a collection of probabilities, $0 < \alpha_{i,j} \leq 1$
 241 with $\alpha_{i,j} = \alpha_{j,i}$, and for an unordered pair $u \neq v$ create an undirected edge between u and v with
 242 probability $\alpha_{i,j}$ if $u \in C_i, v \in C_j$. To turn this undirected graph into a directed graph, we next define
 243 $\{\beta_{i,j}\}_{1 \leq i,j \leq n_c}$ to be a collection of probabilities such that $0 \leq \beta_{i,j} \leq 1$ and $\beta_{i,j} + \beta_{j,i} = 1$. For

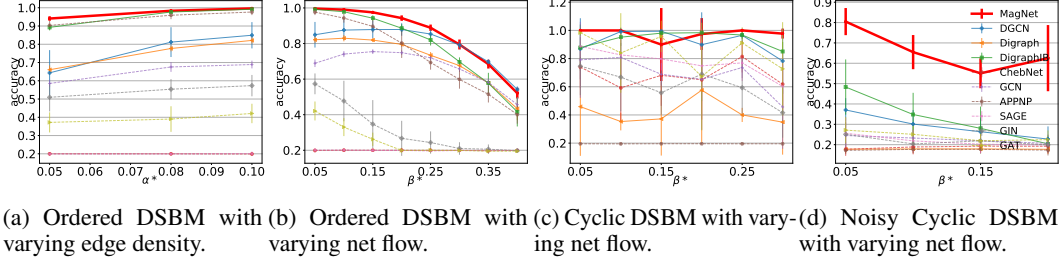
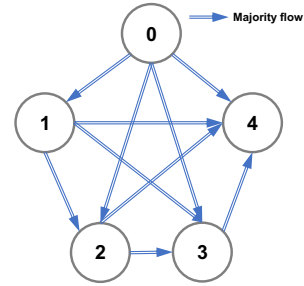


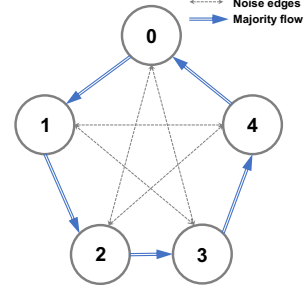
Figure 2: Node classification accuracy. Error bars are one standard error. MagNet is bold red.

each undirected edge $\{u, v\}$, we assign that edge a direction by the rule that the edge points from u to v with probability $\beta_{i,j}$ if $u \in C_i$ and $v \in C_j$, and points from v to u otherwise. We note that if $\alpha_{i,j}$ is constant, then the only way to determine the clusters will be from the directional information.

In Figure 2, we plot the performance of MagNet and other methods on variations of the DSBM. In each of these, we set $n_c = 5$ and the goal is to classify the vertices by cluster. We set $N = 2500$, except in Figure 2a where $N = 500$. In Figure 2a, we plot the performance of our model on the DSBM with $\alpha_{i,j} := \alpha^* = .1, .08, \text{ and } .05$ for $i \neq j$, which varies the density of inter-cluster edges, and set $\alpha_{i,i} = .1$. Here we set $\beta_{i,i} = .5$ and $\beta_{i,j} = .05$ for $i > j$. This corresponds to the ordered meta-graph in Figure 3a. Figure 2b also uses the ordered meta-graph, but here we fix $\alpha_{i,j} = .1$ for all i, j , and set $\beta_{i,j} = \beta^*$, for $i > j$, and allow β^* to vary from .05 to .4, which varies the net flow from one cluster to another. The results in Figure 2c utilize a cyclic meta-graph structure as in Figure 3b (without the gray noise edges). Specifically, we set $\alpha_{i,j} = .1$ if $i = j$ or $i = j \pm 1 \pmod 5$ and $\alpha_{i,j} = 0$ otherwise. We define $\beta_{i,j} = \beta^*$, $\beta_{j,i} = 1 - \beta^*$ when $j = (i - 1) \pmod 5$, and $\beta_{i,j} = 0$ otherwise. In Figure 2d we add noise to the cyclic structure of our meta-graph by setting $\alpha_{i,j} = .1$ for all i, j and $\beta_{i,j} = .5$ for all (i, j) connected by a gray edge in Figure 3b (keeping $\beta_{i,j}$ the same as in Figure 2c for the blue edges).



(a) Ordered meta-graph.



(b) Cyclic meta-graph.

Figure 3: Meta-graphs for the synthetic data sets.

5.1.2 Real datasets

Texas, *Wisconsin*, and *Cornell* are WebKB datasets modeling links between websites at different universities [32]. We use these datasets for both link prediction and node classification with nodes labeled as student, project, course, staff, and faculty in the latter case. *Telegram* [5] is a pairwise influence network between 245 Telegram channels with 8,912 links. To the best of our knowledge, this dataset has not previously been studied in the graph neural network literature. Labels are generated from the method discussed in [5], with a total of four classes. The datasets *Chameleon* and *Squirrel* [33] represent links between Wikipedia pages related to chameleons and squirrels. We use these datasets for link prediction. Likewise, *WikiCS* [28] is a collection of Computer Science articles, which we also use for link prediction. *Cora-ML* and *CiteSeer* are popular citation networks with node labels corresponding to scientific subareas. We use the versions of these datasets provided in [4]. Further details are given in the supplementary material.

5.2 Training and implementation details

Node classification is performed in a semi-supervised setting (i.e., access to the test data, but not the test labels, during training). For the datasets *Cornell*, *Texas*, *Wisconsin*, and *Telegram* we use a 60%/20%/20% training/validation/test split, which might be viewed as more akin to supervised learning, because of the small graph size. For *Cora-ML* and *CiteSeer*, we use the same split as [36]. For all of these datasets we use 10 random data splits. For the DSBM datasets, we generated 5 graphs randomly for each type and for each set of parameters, each with 10 different random node splits.

Table 1: Node classification accuracy. The best results are in **bold** and the second best are underlined.

Type	Method	Cornell	Texas	Wisconsin	Cora-ML	CiteSeer	Telegram
Spectral	ChebNet	79.8±5.0	79.2±7.5	81.6±6.3	80.0±1.8	66.7±1.6	70.2 ±6.8
	GCN	59.0±6.4	58.7±3.8	55.9±5.4	82.0±1.1	66.0±1.5	73.4 ±5.8
Spatial	APPNP	58.7±4.0	57.0±4.8	51.8±7.4	82.6±1.4	66.9±1.8	67.3 ±3.0
	SAGE	<u>80.0±6.1</u>	84.3±5.5	<u>83.1±4.8</u>	<u>82.3±1.2</u>	66.0±1.5	56.6 ±6.0
	GIN	57.9±5.7	65.2±6.5	58.2±5.1	78.1±2.0	63.3±2.5	74.4 ±8.1
	GAT	57.6±4.9	61.1±5.0	54.1±4.2	81.9±1.0	<u>67.3±1.3</u>	72.6 ±7.5
Directed	DGCN	67.3±4.3	71.7±7.4	65.5±4.7	81.3±1.4	66.3±2.0	90.4 ±5.6
	Digraph	66.8±6.2	64.9±8.1	59.6±3.8	79.4±1.8	62.6±2.2	82.0 ±3.1
	DiGraphIB	64.4±9.0	64.9±13.7	64.1±7.0	79.3± 1.2	61.1±1.7	64.1±7.0
This paper	MagNet	84.3±7.0	<u>83.3±6.1</u>	85.7±3.2	79.8±2.5	67.5±1.8	<u>87.6 ±2.9</u>
	Best q	0.25	0.15	0.05	0.0	0.0	0.15

286 We use 20% of the nodes for validation and we vary the proportion of training samples based on the
 287 classification difficulty, using 2%, 10%, and 60% of nodes per class for the ordered, cyclic, and noisy
 288 cyclic DSBM graphs, respectively, during training, and the rest for testing. Hyperparameters were
 289 selected using one of the five generated graphs, and then applied to the other four generated graphs.

290 There are two types of link prediction tasks conducted for performance evaluation. The first type
 291 is to predict the edge direction of pairs of vertices u, v for which either $(u, v) \in E$ or $(v, u) \in E$.
 292 The second type is existence prediction. The model is asked to predict if $(u, v) \in E$ by considering
 293 ordered pairs of vertices (u, v) . For the both types of link prediction, we removed 15% of edges for
 294 testing, 5% for validation, and use the rest of the edges for training. The connectivity was maintained
 295 during splitting. 10 splits were generated randomly for each graph and the input features are in-degree
 296 and out-degree of nodes. Full details are provided in the supplementary material.

297 In all experiments, we used the normalized magnetic Laplacian and implement MagNet with con-
 298 volution defined as in (4), meaning that our network may be viewed as the magnetic Laplacian
 299 generalization of ChebNet. We compare with multiple baselines in three categories: (i) spectral
 300 methods: ChebNet [13], GCN [22]; (ii) spatial methods: APPNP [23], SAGE [20], GIN [41], GAT
 301 [38]; and (iii) methods designed for directed graphs: DGCN [37], and two variants of [36], a basic
 302 version (DiGraph) and a version with higher order inception blocks (DiGraphIB). All baselines in the
 303 experiments have two graph convolutional layers, except for the node classification on the DSBM
 304 using the cyclic meta-graphs (Figures 2c, 2d, and 3b) for which we also tested three layers during the
 305 grid search. For ChebNet, we use the symmetrized adjacency matrix. For the spatial networks we
 306 apply both the symmetrized and asymmetric adjacency matrix for node classification. The results
 307 reported are the better of the two results. Full details are provided in the supplemental material.

308 5.3 Results

309 We see that MagNet performs well across all tasks. As indicated in Table 1, our cross-validation
 310 procedure selects $q = 0$ for node classification on the citation networks *Cora-ML* and *CiteSeer*.
 311 This means we achieved the best performance when regarding directional information as noise,
 312 suggesting symmetrization-based methods are appropriate in the context of node classification on
 313 citation networks. This matches our intuition. For example, in *Cora-ML*, the task is to classify
 314 research papers by scientific subarea. If the topic of a given paper is “machine learning,” then it is
 315 likely to both cite and be cited by other machine learning papers. For all other datasets, we find
 316 the optimal value of q is nonzero, indicating that directional information is important. Our network
 317 exhibits the best performance on three out of six of these datasets and is a close second on *Texas* and
 318 *Telegram*. We also achieve an at least four percentage point improvement over both ChebNet and
 319 GCN on the four data sets for which $q > 0$. These networks are similar to ours but with the classical
 320 graph Laplacian. This isolates the effects of the magnetic Laplacian and shows that it is a valuable
 321 tool for encoding directional information. MagNet also compares favorably to non-spectral methods
 322 on the WebKB networks (*Cornell*, *Texas*, *Wisconsin*). Indeed, MagNet obtains a $\sim 4\%$ improvement

Table 2: Link prediction accuracy. The best results are in **bold** and the second best are underlined.

	Direction prediction				Existence prediction			
	Cornell	Wisconsin	Cora-ML	CiteSeer	Cornell	Wisconsin	Cora-ML	CiteSeer
ChebNet	71.0±5.5	67.5±4.5	72.7±1.5	68.0±1.6	80.1±2.3	82.5±1.9	80.0±0.6	77.4±0.4
GCN	56.2±8.7	71.0±4.0	79.8±1.1	68.9±2.8	75.1±1.4	75.1±1.9	81.6±0.5	76.9±0.5
APPNP	69.5±9.0	75.1±3.5	<u>83.7±0.7</u>	77.9±1.6	74.9±1.5	75.7±2.2	<u>82.5±0.6</u>	78.6±0.7
SAGE	75.2±11.0	72.0±3.5	68.2±0.8	68.7±1.5	79.8±2.4	77.3±2.9	75.0±0.0	74.1±1.0
GIN	69.3±6.0	74.8±3.7	83.2±0.9	76.3±1.4	74.5±2.1	76.2±1.9	<u>82.5±0.7</u>	77.9±0.7
GAT	67.9±11.1	53.2±2.6	50.0±0.1	50.6±0.5	77.9±3.2	74.6±0.0	75.0±0.0	75.0±0.0
DGCN	80.7±6.3	74.5±7.2	79.6±1.5	78.5±2.3	80.0±3.9	<u>82.8±2.0</u>	82.1±0.5	<u>81.2±0.4</u>
DiGraph	79.3±1.9	<u>82.3±4.9</u>	80.8±1.1	81.0±1.1	80.6±2.5	<u>82.8±2.6</u>	81.8±0.5	82.2±0.6
DiGraphIB	79.8±4.8	82.0±4.9	83.4±1.1	<u>82.5±1.3</u>	<u>80.5±3.6</u>	82.4±2.2	82.2±0.5	81.0±0.5
MagNet	80.7±2.7	83.6±2.8	86.1±0.9	85.1±0.8	80.6±3.8	82.9±2.6	82.8±0.7	79.9±0.5
Best q	0.10	0.05	0.05	0.15	0.25	0.25	0.05	0.05

323 on *Cornell* and a $\sim 2.5\%$ improvement on *Wisconsin*, while on *Texas* it has the second best accuracy,
 324 close behind SAGE. We also see the other directed methods have relatively poor performance on the
 325 WebKB networks, perhaps since these graphs are fairly small and have very few training samples.

326 On the DSBM, as illustrated in Figure 2, we see that MagNet generally performs quite well and is the
 327 best performing network in the vast majority cases (for full details, see Section 7 of the supplement).
 328 The networks DGCN and DiGraphIB rely on second order proximity matrices. As demonstrated
 329 in Figure 2c, these methods are well suited for networks with a cyclic meta-graph structure since
 330 nodes in the same cluster are likely to have common neighbors. MagNet, on the other hand, does not
 331 use second-order proximity, but can still learn the clusters by stacking multiple layers together. This
 332 improves MagNet’s ability to adapt to directed networks with different underlying topologies. This is
 333 illustrated in Figure 2d where the network has an approximately cyclic meta-graph structure. In this
 334 setting, MagNet continues to perform well, but the performance of DGCN and DiGraphIB deteriorate
 335 significantly. Interestingly, MagNet performs well on the DSBM cyclic meta-graph (Figure 2c)
 336 with $q \approx .1$, whereas $q \geq .2$ is preferred for the other three DSBM tests; we leave a more in-depth
 337 investigation for future work. Further details are available in Section 8 of the supplement.

338 For link prediction, we achieve the best performance on seven out of eight tests as shown in Table
 339 2. We also note that Table 2 reports optimal non-zero q values for each task. This indicates that
 340 incorporating directional information is important for link prediction, even on citation networks such
 341 as *Cora* and *CiteSeer*. This matches our intuition, since there is a clear difference between a paper
 342 with many citations and one with many references.

343 6 Conclusion

344 We have introduced MagNet, a neural network for directed graphs based on the magnetic Laplacian.
 345 This network can be viewed as the natural extension of spectral graph convolutional networks to
 346 the directed graph setting. We demonstrate the effectiveness of our network, and the importance
 347 of incorporating directional information via a complex Hermitian matrix, for link prediction and
 348 node classification on both real and synthetic datasets. Interesting avenues of future research would
 349 be using multiple q ’s along different channels, exploring the role of different normalizations of the
 350 magnetic Laplacian, and to incorporating the magnetic Laplacian into other network architectures.

351 **Limitations and Ethical Considerations:** Our method has natural extensions to weighted, directed
 352 graphs when all edges are directed. However, it not clear what is the best way to extend it to weighted
 353 mixed graphs (with both directed and undirected edges). Our network does not incorporate an
 354 attention mechanism and, similar to many other networks, is not scalable to large graphs in its current
 355 form (although this may be addressed in future work). All of our data is publicly available for research
 356 purposes and does not contain personally identifiable information or offensive content. The method
 357 presented here has no greater or lesser impact on society than other graph neural network algorithms.

References

- 358
- 359 [1] James Atwood and Don Towsley. Diffusion-convolutional neural networks. In D. Lee,
360 M. Sugiyama, U. Luxburg, I. Guyon, and R. Garnett, editors, Advances in Neural Information
361 Processing Systems, volume 29, pages 1993–2001. Curran Associates, Inc., 2016.
- 362 [2] Mikhail Belkin and Partha Niyogi. Laplacian eigenmaps for dimensionality reduction and data
363 representation. Neural computation, 15(6):1373–1396, 2003.
- 364 [3] Austin R Benson, David F Gleich, and Jure Leskovec. Higher-order organization of complex
365 networks. Science, 353(6295):163–166, 2016.
- 366 [4] Aleksandar Bojchevski and Stephan Günnemann. Deep gaussian embedding of graphs: Un-
367 supervised inductive learning via ranking. In ICLR Workshop on Representation Learning on
368 Graphs and Manifolds, 2017.
- 369 [5] Alexandre Bovet and Peter Grindrod. The activity of the far right on tele-
370 gram. [https://www.researchgate.net/publication/346968575_The_Activity_](https://www.researchgate.net/publication/346968575_The_Activity_of_the_Far_Right_on_Telegram_v21)
371 [of_the_Far_Right_on_Telegram_v21](https://www.researchgate.net/publication/346968575_The_Activity_of_the_Far_Right_on_Telegram_v21), 2020.
- 372 [6] Joan Bruna, Wojciech Zaremba, Arthur Szlam, and Yann LeCun. Spectral networks and deep
373 locally connected networks on graphs. In International Conference on Learning Representations
374 (ICLR), 2014.
- 375 [7] Fan Chung. Laplacians and the cheeger inequality for directed graphs. Annals of Combinatorics,
376 9(1):1–19, 2005.
- 377 [8] Fan Chung and Mark Kempton. A local clustering algorithm for connection graphs. In
378 International Workshop on Algorithms and Models for the Web-Graph, pages 26–43. Springer,
379 2013.
- 380 [9] Fan RK Chung and Fan Chung Graham. Spectral graph theory. Number 92. American
381 Mathematical Soc., 1997.
- 382 [10] Alexander Cloninger. A note on markov normalized magnetic eigenmaps. Applied and
383 Computational Harmonic Analysis, 43(2):370 – 380, 2017.
- 384 [11] Ronald R Coifman and Stéphane Lafon. Diffusion maps. Applied and computational harmonic
385 analysis, 21(1):5–30, 2006.
- 386 [12] Mihai Cucuringu, Huan Li, He Sun, and Luca Zanetti. Hermitian matrices for clustering directed
387 graphs: insights and applications. In International Conference on Artificial Intelligence and
388 Statistics, pages 983–992. PMLR, 2020.
- 389 [13] Michaël Defferrard, Xavier Bresson, and Pierre Vandergheynst. Convolutional neural networks
390 on graphs with fast localized spectral filtering. In Advances in Neural Information Processing
391 Systems 29, pages 3844–3852, 2016.
- 392 [14] David K Duvenaud, Dougal Maclaurin, Jorge Iparraguirre, Rafael Bombarell, Timothy Hirzel,
393 Alan Aspuru-Guzik, and Ryan P Adams. Convolutional networks on graphs for learning
394 molecular fingerprints. In C. Cortes, N. Lawrence, D. Lee, M. Sugiyama, and R. Garnett,
395 editors, Advances in Neural Information Processing Systems, volume 28, pages 2224–2232.
396 Curran Associates, Inc., 2015.
- 397 [15] Bruno Messias F. de Resende and Luciano da F. Costa. Characterization and comparison of large
398 directed networks through the spectra of the magnetic laplacian. Chaos: An Interdisciplinary
399 Journal of Nonlinear Science, 30(7):073141, 2020.
- 400 [16] Michaël Fanuel, Carlos M. Alaíz, Ángela Fernández, and Johan A.K. Suykens. Magnetic
401 eigenmaps for the visualization of directed networks. Applied and Computational Harmonic
402 Analysis, 44:189–199, 2018.
- 403 [17] Michaël Fanuel, Carlos M Alaiz, and Johan AK Suykens. Magnetic eigenmaps for community
404 detection in directed networks. Physical Review E, 95(2):022302, 2017.

- 405 [18] Satoshi Furutani, Toshiki Shibahara, Mitsuaki Akiyama, Kunio Hato, and Masaki Aida. Graph
406 signal processing for directed graphs based on the hermitian laplacian. In Machine Learning
407 and Knowledge Discovery in Databases, pages 447–463, 2020.
- 408 [19] Krystal Guo and Bojan Mohar. Hermitian adjacency matrix of digraphs and mixed graphs.
409 Journal of Graph Theory, 85(1):217–248, 2017.
- 410 [20] William L. Hamilton, Rex Ying, and Jure Leskovec. Inductive representation learning on large
411 graphs. In Proceedings of the 31st International Conference on Neural Information Processing
412 Systems, NIPS’17, page 1025–1035, Red Hook, NY, USA, 2017. Curran Associates Inc.
- 413 [21] David K Hammond, Pierre Vandergheynst, and Rémi Gribonval. Wavelets on graphs via spectral
414 graph theory. Applied and Computational Harmonic Analysis, 30(2):129–150, 2011.
- 415 [22] Thomas N. Kipf and Max Welling. Semi-supervised classification with graph convolutional
416 networks. In International Conference on Learning Representations (ICLR), 2017.
- 417 [23] Johannes Klicpera, Aleksandar Bojchevski, and Stephan Günnemann. Predict then propagate:
418 Graph neural networks meet personalized pagerank. In ICLR, 2019.
- 419 [24] Ron Levie, Wei Huang, Lorenzo Bucci, Michael M Bronstein, and Gitta Kutyniok. Trans-
420 ferability of spectral graph convolutional neural networks. arXiv preprint arXiv:1907.12972,
421 2019.
- 422 [25] Elliott H Lieb and Michael Loss. Fluxes, laplacians, and kasteleyn’s theorem. In Statistical
423 Mechanics, pages 457–483. Springer, 1993.
- 424 [26] Yi Ma, Jianye Hao, Yaodong Yang, Han Li, Junqi Jin, and Guangyong Chen. Spectral-based
425 graph convolutional network for directed graphs. arXiv:1907.08990, 2019.
- 426 [27] Antonio G Marques, Santiago Segarra, and Gonzalo Mateos. Signal processing on directed
427 graphs: The role of edge directionality when processing and learning from network data. IEEE
428 Signal Processing Magazine, 37(6):99–116, 2020.
- 429 [28] Péter Mernyei and Cătălina Cangea. Wiki-cs: A wikipedia-based benchmark for graph neural
430 networks. arXiv preprint arXiv:2007.02901, 2020.
- 431 [29] Bojan Mohar. A new kind of hermitian matrices for digraphs. Linear Algebra and its
432 Applications, 584:343–352, 2020.
- 433 [30] Federico Monti, Karl Otness, and Michael M. Bronstein. Motifnet: A motif-based graph
434 convolutional network for directed graphs. In 2018 IEEE Data Science Workshop, pages
435 225–228, 2018.
- 436 [31] Antonio Ortega, Pascal Frossard, Jelena Kovačević, José MF Moura, and Pierre Vandergheynst.
437 Graph signal processing: Overview, challenges, and applications. Proceedings of the IEEE,
438 106(5):808–828, 2018.
- 439 [32] Hongbin Pei, Bingzhe Wei, Kevin Chen-Chuan Chang, Yu Lei, and Bo Yang. Geom-gcn:
440 Geometric graph convolutional networks. arXiv preprint arXiv:2002.05287, 2020.
- 441 [33] Benedek Rozemberczki, Carl Allen, and Rik Sarkar. Multi-scale attributed node embedding.
442 arXiv preprint arXiv:1909.13021, 2019.
- 443 [34] Jianbo Shi and Jitendra Malik. Normalized cuts and image segmentation. In Proceedings of
444 IEEE computer society conference on computer vision and pattern recognition, pages 731–737.
445 IEEE, 1997.
- 446 [35] Daniel A Spielman and Shang-Hua Teng. Nearly-linear time algorithms for graph partitioning,
447 graph sparsification, and solving linear systems. In Proceedings of the thirty-sixth annual ACM
448 symposium on Theory of computing, pages 81–90, 2004.
- 449 [36] Z. Tong, Yuxuan Liang, Changsheng Sun, Xinke Li, David S. Rosenblum, and A. Lim. Digraph
450 inception convolutional networks. In NeurIPS, 2020.

- 451 [37] Zekun Tong, Yuxuan Liang, Changsheng Sun, David S. Rosenblum, and Andrew Lim. Directed
452 graph convolutional network. [arXiv:2004.13970](https://arxiv.org/abs/2004.13970), 2020.
- 453 [38] Petar Veličković, Guillem Cucurull, Arantxa Casanova, Adriana Romero, Pietro Liò, and Yoshua
454 Bengio. Graph Attention Networks. [International Conference on Learning Representations](https://arxiv.org/abs/1710.10903),
455 2018.
- 456 [39] Palmer W.R. and Zheng T. Spectral clustering for directed networks. [Studies in Computational
457 Intelligence](https://arxiv.org/abs/2105.08227), 943, 2021.
- 458 [40] Zonghan Wu, Shirui Pan, Fengwen Chen, Guodong Long, Chengqi Zhang, and Philip S. Yu. A
459 comprehensive survey on graph neural networks. [IEEE Transactions on Neural Networks and
460 Learning Systems](https://arxiv.org/abs/2004.03578), 32(1):4–24, 2020.
- 461 [41] Keyulu Xu, Weihua Hu, Jure Leskovec, and Stefanie Jegelka. How powerful are graph neural
462 networks? [arXiv preprint arXiv:1810.00826](https://arxiv.org/abs/1810.00826), 2018.
- 463 [42] Jie Zhou, Ganqu Cui, Zhengyan Zhang, Cheng Yang, Zhiyuan Liu, Lifeng Wang, Changcheng
464 Li, and Maosong Sun. Graph neural networks: A review of methods and applications. [arXiv
465 preprint arXiv:1812.08434](https://arxiv.org/abs/1812.08434), 2018.

466 Checklist

- 467 1. For all authors...
- 468 (a) Do the main claims made in the abstract and introduction accurately reflect the paper’s
469 contributions and scope? [\[Yes\]](#)
- 470 (b) Did you describe the limitations of your work? [\[Yes\]](#) Please see Section 6.
- 471 (c) Did you discuss any potential negative societal impacts of your work? [\[Yes\]](#) Please see
472 Section 6.
- 473 (d) Have you read the ethics review guidelines and ensured that your paper conforms to
474 them? [\[Yes\]](#)
- 475 2. If you are including theoretical results...
- 476 (a) Did you state the full set of assumptions of all theoretical results? [\[Yes\]](#) Please see
477 Section 5 of the supplement.
- 478 (b) Did you include complete proofs of all theoretical results? [\[Yes\]](#) Please see Section 5
479 of the supplement.
- 480 3. If you ran experiments...
- 481 (a) Did you include the code, data, and instructions needed to reproduce the main exper-
482 imental results (either in the supplemental material or as a URL)? [\[Yes\]](#) Please see
483 Section 1 of the supplemental material.
- 484 (b) Did you specify all the training details (e.g., data splits, hyperparameters, how they were
485 chosen)? [\[Yes\]](#) Please see Section 5 of the main text and Section 3 of the supplemental
486 material.
- 487 (c) Did you report error bars (e.g., with respect to the random seed after running experi-
488 ments multiple times)? [\[Yes\]](#) Please see Section 5 of the main text and Section 7 of the
489 supplemental material.
- 490 (d) Did you include the total amount of compute and the type of resources used (e.g.,
491 type of GPUs, internal cluster, or cloud provider)? [\[Yes\]](#) Please see Section 3 of the
492 supplemental material.
- 493 4. If you are using existing assets (e.g., code, data, models) or curating/releasing new assets...
- 494 (a) If your work uses existing assets, did you cite the creators? [\[Yes\]](#) Please see Section 5
495 of the main text, the supplemental material, and the anonymous code for this paper that
496 lists all used packages.
- 497 (b) Did you mention the license of the assets? [\[Yes\]](#) Please see our anonymous code for
498 this paper.

- 499 (c) Did you include any new assets either in the supplemental material or as a URL? [Yes]
500 Please see our anonymous code for this paper.
- 501 (d) Did you discuss whether and how consent was obtained from people whose data you're
502 using/curating? [Yes] All data is publicly available and permits use for research.
- 503 (e) Did you discuss whether the data you are using/curating contains personally identifiable
504 information or offensive content? [Yes] All data, to the best of our knowledge, is de-
505 identified and contains no personal information, nor does it contain offensive content.
- 506 5. If you used crowdsourcing or conducted research with human subjects...
- 507 (a) Did you include the full text of instructions given to participants and screenshots, if
508 applicable? [N/A]
- 509 (b) Did you describe any potential participant risks, with links to Institutional Review
510 Board (IRB) approvals, if applicable? [N/A]
- 511 (c) Did you include the estimated hourly wage paid to participants and the total amount
512 spent on participant compensation? [N/A]